COMBINED MACRO-MESO SCALE MODELING OF SINTERING. PART I: CONTINUUM APPROACH

Eugene A. Olevsky
Department of Mechanical Engineering, San Diego State University
5500 Campanile Dr., CA 92182-1323, USA

Veena Tikare
Sandia National Laboratories
Albuquerque, NM 87107, USA

ABSTRACT: An integrated approach, including a continuum theory of sintering and mesostructure evolution analysis, is used for the solution of the problem of bi-layered structure sintering. Two types of bi-layered structures are considered: layers of the same material different by initial porosity, and layers of two different materials. The effective sintering stress and the normalized bulk modulus for the bi-layer powder sintering are derived based on mesoscale simulations. The combined effect of the layers' porosity and differences in sintering rate on shrinkage and warpage is studied for both sintering on a rigid substrate and free sintering.

1. INTRODUCTION

A continuum theory of sintering has been intensively developed over the last decade. This modeling approach enabled realistic description of the macroscopic behavior of porous and powder materials subjected to densification (treatment by pressure and sintering), including analysis of macroscopic shape evolution and spatial distribution of stresses, strains and density. The accuracy of the modeling results depends on the correctness of the constitutive parameters employed by the continuum theory of sintering. Among those are the sintering stress and the bulk and shear moduli of material resistance.

The present work is an attempt to link two different levels of material description: meso and macro, thereby enabling a new continuum-structural modeling approach. The above-mentioned material constitutive parameters (in particular, the effective sintering stress, and the bulk modulus) are determined by a mesoscale Monte-Carlo simulation of the sintering of a 2-D grain structure (described in details in a companion paper [1]). These parameters are considered to be functions of one structure characteristics - porosity.

The obtained values are substituted into a finite-element code based on the continuum model of sintering. Here we demonstrate the usage of this code for modeling of sintering of bi-layered ceramic composites.

2. DETERMINATION OF CONSTITUTIVE PARAMETERS

In accordance with the continuum theory of sintering [2], the mechanical response of a nonlinear-viscous porous body subjected to sintering and an external load can be described by a rheological (constitutive) relationship connecting components of stress tensor σ_{ij} and strain rate tensor $\dot{\varepsilon}_{ij}$:

$$\sigma_{ij} = \frac{\sigma(W)}{W}\left[\varphi\dot{\varepsilon}_{ij} + \left(\psi - \frac{1}{3}\varphi\right)\dot{\varepsilon}\delta_{ij}\right] + P_L\delta_{ij} \qquad (1)$$

DISCLAIMER

DISCLAIMER

Portions of this document may be illegible in electronic image products. Images are produced from the best available original document.

where W is the so-called "equivalent strain rate", and $\sigma(W)$ is the "equivalent stress"; φ and ψ are the shear and bulk viscosity module, which depend on porosity θ (for example, following [3], $\varphi = (1-\theta)^2$, $\psi = \frac{2}{3}\frac{(1-\theta)^3}{\theta}$); δ_{ij} is a Kronecker symbol ($\delta_{ij} = 1$ if i=j and $\delta_{ij} = 0$ if $i \neq j$); $\dot{e}$ is the first invariant of the strain rate tensor, *i.e.* sum of tensor diagonal components: $\dot{e} = \dot{\varepsilon}_{11} + \dot{\varepsilon}_{22} + \dot{\varepsilon}_{33}$.

The porosity θ is defined as $1 - \frac{\rho}{\rho_T}$, where ρ and ρ_T relative and theoretical (corresponding to a fully-dense state) densitites, respectively. Physically, $\dot{e}$ represents the volume change rate of a porous body.

Equivalent strain rate W is connected with the current porosity and with the invariants of the strain rate tensor:

$$W = \frac{1}{\sqrt{1-\theta}}\sqrt{\varphi\dot{\gamma}^2 + \psi\dot{e}^2} \tag{2}$$

$\dot{\gamma}$ is the second invariant of the strain rate tensor deviator and represents, physically, the shape change rate of a porous body:

$$\dot{\gamma} = \left[\left(\dot{\varepsilon}_{ij} - \frac{1}{3}\dot{e}\delta_{ij}\right)\left(\dot{\varepsilon}_{ij} - \frac{1}{3}\dot{e}\delta_{ij}\right)\right]^{1/2} \tag{3}$$

Physically, $\dot{\gamma}$ represents the shape change rate of a porous body. It can be expressed in terms of the main elongation rates: $\dot{\varepsilon}_1, \dot{\varepsilon}_2, \dot{\varepsilon}_3$:

$$\dot{\gamma} = \frac{1}{\sqrt{3}}\sqrt{(\dot{\varepsilon}_1 - \dot{\varepsilon}_2)^2 + (\dot{\varepsilon}_2 - \dot{\varepsilon}_3)^2 + (\dot{\varepsilon}_3 - \dot{\varepsilon}_1)^2} \tag{4}$$

$\sigma(W)$ determines the constitutive behavior of a porous material. If $\sigma(W)$ is described by the linear relationship: $\sigma(W) = 2\eta_0 W$, where η_0 is the shear viscosity of a fully-dense material, one obtains the equation corresponding to the behavior of a linear-viscous porous body:

$$\sigma_{ij} = 2\eta_o\left[\varphi\dot{\varepsilon}_{ij} + \left(\psi - \frac{1}{3}\varphi\right)\dot{e}\delta_{ij}\right] + P_L\delta_{ij} \tag{5}$$

P_L is an effective sintering stress.

In the constitutive relationship (1), three main parameters P_L, φ, and ψ should be determined as functions of porosity.

Effective sintering stress

In the framework of the continuum theory of sintering, the effective Laplace pressure (sintering stress) P_L is defined:

$$P_L = \frac{\partial F}{\partial \vartheta} \tag{6}$$

where F is a free surface energy, and ϑ is a porous volume subjected to sintering.

Effective sintering stress corresponds to the result of the collective action of local capillary stresses in a porous material. The relationship between the effective and local Laplace pressure depends on the procedure of averaging of the above mentioned local stresses over a macroscopic porous volume.

A question of the determination of the effective Laplace pressure ("sintering stress", "sintering potential", "sintering (driving) force") has been studied by many authors [].

Skorohod [3] suggested a stochastic approach for determination of the effective Laplace pressure.

Beere [4] determined the "driving force for sintering" as the difference in vacancy concentrations at the pore surface and the grain boundary. The sintering force in this model can be expressed as a function of porosity through the dependence between pore volume fraction and dihedral angle between grain surfaces. The expressions for the sintering force were obtained for the volume and grain boundary diffusion mechanisms. Here the sintering force is inversely proportional to the grain size.

Bordia and Scherer [5] demonstrated that, for linear-viscous models, the effective Laplace pressure can be expressed as a product of the volume shrinkage rate and the effective bulk viscosity. Thus, the effective Laplace pressure can be derived for the models which provide explicit relationships for these two values.

Rahaman *et al.* [6] obtained an expression for the sintering stress using the Zener relation. The sintering stress is represented as the ratio between surface tension and the product of the grain size and porosity. Thus, in the framework of this model, the sintering stress increases with density for a fixed grain size. However, the experiments on sintering of CdO powder indicated the decrease of the sintering stress with increasing density when grain growth occurs (which is in agreement with the results of Beere [4]).

Hsueh *et al.* [7], using a visco-elastic analysis and based upon experimental data for hot pressing experiments of Al_2O_3 powder, came to the conclusion of the constancy of the sintering stress. It should be noted, that hot pressing involves additional factors in comparison with free sintering (such as friction forces, for example) which can be a reason for the deviation of these results from those obtained by Beere [4] and Rahaman *et al.* [6].

De Jonghe and Rahaman [8] determined the thermodynamic meaning of the sintering stress for two-dimensional porous bodies. They postulated that the sintering stress for a densifying powder compact can be considered as an equivalent applied stress that would produce the same densification rate for the system, at identical geometry but with surface tension effects absent. Basically, this definition is limited by the case of homogeneous porous material.

Ashby [9] introduced two expressions for the effective Laplace pressure considering two stages of sintering (see Fig.1). At the first stage (when the relative density is not higher than 92%), an open character of porosity prevails. Here, for the derivation of the effective Laplace pressure, the expression for the average contact area as a function of the relative density is used. At the second stage, pores are separated. Here the effective Laplace pressure is defined as a ratio of the double surface tension and the pore radius. The expression for the dependence of the pore radius on the relative density (obtained by Swinkels and Ashby [10]) is substituted into the relationship for the effective Laplace pressure which, thus, becomes a function of the relative density as well. For both stages, the effective Laplace pressure increases with the increase of the relative density. These results have been modified by Cocks [11] who introduced an additional item responsible for the increase in grain boundary area.

Later, the expression for the effective sintering stress (sintering potential) was derived for the different controlling mechanisms of material flow under sintering.

McMeeking and Kuhn [12] and Bouvard and McMeeking [13] developed a relationship for the effective Laplace pressure for diffusion controlled creep at the earlier (first) stage of sintering. Here the effective Laplace pressure increases with the increase of the relative density. This result is also modified by Cocks [11] by introduction of an additional term responsible for the increase in grain boundary area.

Besson and Abouaf [14] noted that that the dependence of the effective Laplace pressure on the relative density seems to be related to the material, processing (cold compaction) and testing conditions.

Cocks and Aparicio [15] defined the effective "sintering force" as the applied force which provides the stress field which is in equilibrium with this force and surface tension and satisfies the boundary condition for the capillary stresses at the pore surface while stress gradients are absent at the pore surface.

Riedel, Svoboda *et al.* in a series of works [16,17,18] elaborated models of sintering with diffusional creep (grain boundary) as a controlling mechanism of material flow. The expressions for effective sintering stress include the specific grain boundary energy [16], the interparticle neck geometrical parameters [17], and the contribution of the solid-liquid interface energy (in the case of liquid-phase sintering) [18]. Here the effective sintering stress increases with increasing relative density for large values of the dihedral angle between grain surfaces and decreases with increasing relative density for small values of the dihedral angle.

For the determination of the effective sintering stress, we use an original approach based upon mesoscale simulations of sintering of a 2-D unit-cell. At each step of the meso-structure evolution the shrinking volume and the free surface of a rectangular unit cell with a random grain-pore arrangement represented in Fig. 1 are calculated. Then the effective sintering stress is determined using relationship (6). The details of the corresponding simulations are described in a companion paper [1]. As a result, the dependence effective sintering stress – relative density is obtained (Fig. 2).

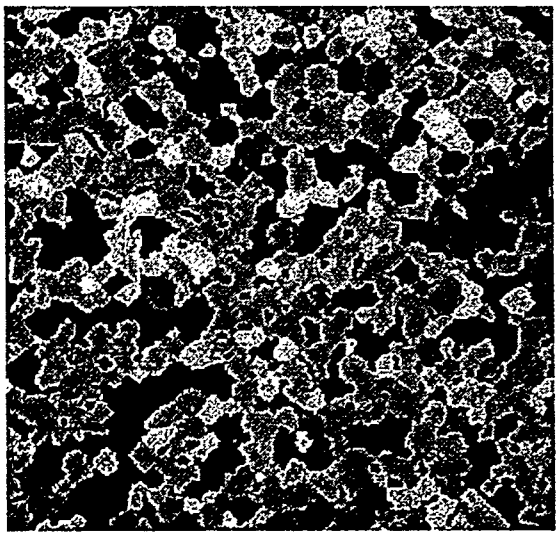

Fig. 1 Random mesoscale structure

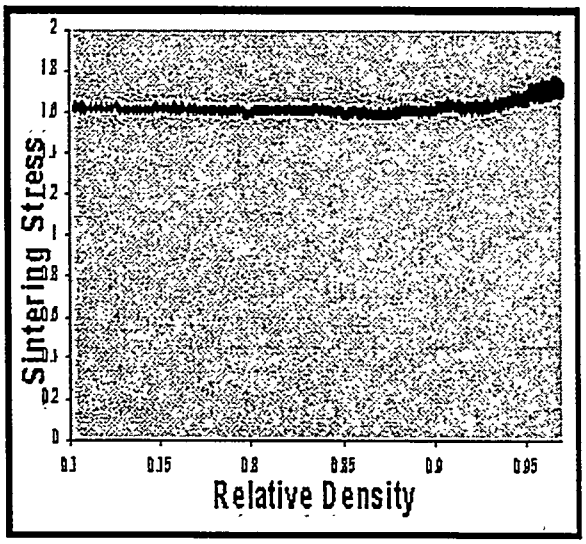

Fig. 2 Dependence of the effective sintering stress on porosity as a result of the mesoscale simulations

Applying regression analysis (see Ref. [1]), the following analytical expression for the effective sintering stress as a function of porosity is revealed:

$$\overline{P}_L = 1.7(1-\theta)^{0.26} \tag{7}$$

Effective normalized bulk modulus.

For the determination of the porous materials' bulk modulus ψ, a considerable amount of work has been carried out by many authors (see, for example, for linear-viscous materials [3,9,19-23] and, for materials with power-law creep properties, [24-27]).

In particular, both Mackenzie [28] and Skorohod [3], used a hydrodynamic analogy of the theory of elasticity to find the bulk modulus of a unit cell containing one spherical pore. Mackenzie considered a three layer design of such a unit cell, when the pore is surrounded by a spherical layer of a fully-dense material, which, in turn, is embodied in the medium with effective properties. Skorohod considered a spherical pore surrounded by an effective porous layer and employed a self-consistent approach to find the effective bulk modulus.

Using the results describing the kinetics of shrinkage and the dependence of the effective sintering stress on porosity obtained on the basis of mesoscale simulations one can determine the effective bulk modulus (see companion paper [1]). The corresponding regression analysis of the numerical data enables the following analytical expression for ψ:

$$\psi = \frac{2}{3}\frac{(1-\theta)^{2.23}}{\theta^{1.12}} \tag{8}$$

3. SOLUTION OF THE PROBLEM OF SINTERING OF BI-LAYERED CERAMIC COMPOSITES

The growth in radio frequency (RF) wireless communication appliances (cell phones, pagers, PDAs, GPS, etc.) is creating a significant opportunity for multilayer ceramic technology to integrate RF circuitry/components required for these applications. However, the densification/sintering behavior of composite "layered" material systems is not well understood and cofire (co-sintering) capability is largely determined by experimental methods. Progress in the integration of these layered material systems will be greatly enhanced by the development of materials and process models that can encompass the densification/sintering behavior - much as modeling has enhanced the development of advanced semiconductor integrated devices. When incorporated in a finite-element code, the continuum theory of sintering allows the solution of one of the most important problems of co-firing multilayer ceramic composites - it can predict warpage caused by differential sintering.

In the case of linear-viscous properties of the porous body skeleton, the finite-element approximation of equation (5) is immediately reduced to the solution of a set of linear equations relative to unknown nodal velocities. Using the conventional finite-element analysis designations, one can represent this set in the form:

$$\left[\int_{\vartheta}[B]^T[D][B]d\vartheta\right]\{V_n\} = -\int_{\vartheta}[B]^T P_L\{1\}d\vartheta \tag{9}$$

where [B] is the matrix correlating the strain rates with the nodal velocities V_n; [D] is the matrix correlating the stresses with the strain rates ("matrix of viscosities"); ϑ is a macroscopic porous volume under investigation; g is the gravity acceleration. The right-hand part of the latter equation represents the nodal forces. In the case of uniform distribution of material properties in the volume ϑ, the nodal forces associated with the sintering stress P_L (the first term in the right-hand part of Eq. (9)) will be equal to zero everywhere except of the nodes which belong to the external boundary of ϑ. The multiplier $\left[\int_{\vartheta}[B]^T[D][B]d\vartheta\right]$ in the left-hand part corresponds to the coefficients in the set of linear equations (9) relative to the unknown nodal velocities V_n.

The effective sintering stress and the effective normalized bulk modulusare used in accordance with expressions (7) and (8). The effective normalized shear modulus is employed in conformity to the Skorohod model [3]:

$$\overline{P}_L = (1-\theta)^2 \tag{10}$$

After the solution of set (9), the field of strain rates is calculated. The new values of relative densities are calculated using the continuity equation for each finite element:

$$\frac{\dot{\theta}}{1-\theta} = \dot{e} \tag{11}$$

The above-mentioned finite-element algorithm is implemented for the solution of three problems of sintering of bi-layer structures.

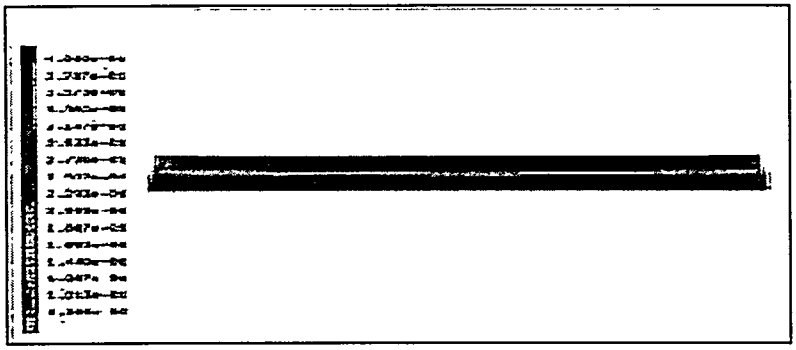

Fig. 3 Sintering of a bi-porous structure on a rigid substrate.
Porosity distribution. Initial porosities are 40% -top layer, 20% - bottom layer

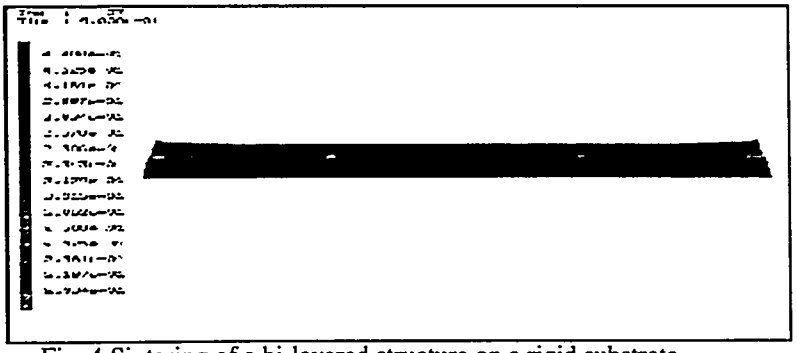

Fig. 4 Sintering of a bi-layered structure on a rigid substrate.
Porosity distribution. Initial porosities are 40%, sintering stress ratio is 1:50

The first two problems are related to sintering on a rigid substrate: the first is sintering of a bi-porous structure (initial porosities are 40 % for the top layer and 20% for the bottom layer) with the same chemical composition of the two layers, the second problem is sintering of a bi-layer structure with layers of the same initial porosity (40%) and different shrinkage rates (sintering stress ratio is accepted to be 1:50). The results of the modeling are shown in Figs. 3 and 4, respectively. In both cases the densification front propagates starting from the top periphery areas which assume the highest density. The bottom periphery zones have the highest porosity due to the imposed constrain from the rigid substrate. In both cases a porous core is formed in the top layer. With respect to the character of the densification front propagation, some difference between the solution of these two problems is observed. In the case of the bi-porous structure, the interface boundary serves as an initial source for the densification wave, while the bi-layer with differences in chemical composition maintains a self-similar density (porosity) spatial distribution in the bottom layer.

The undertaken "computer experiments" indicate that, by and large, difference in chemical composition of adjacent layers has stronger impact on the development of stress and density gradients in comparison with difference in porosity.

The last of the above-mentioned three problems is related to free sintering of a bi-layer structure with the uniform initial distribution of porosity (40%) and with different shrinkage rates for the two layers. The ratio of the effective sintering stresses is assumed to be 1: 50. Fig. 5 shows a 3-D image of the sintered cylindrical bi-layer specimen with its porosity spatial distribution. Due to the difference in shrinkage rates, the top layer contracts faster, causing the pronounced bending of the specimen.

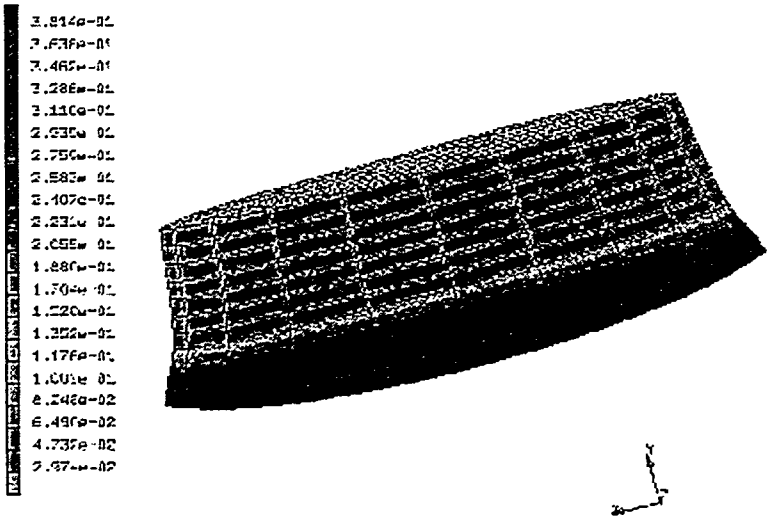

Fig. 5 Free sintering of a bi-layered structure. Poosity distribution.
Initial porosities are 40%, sintering stress ratio is 1:50

3. CONCLUSIONS

- The success of modeling at the macroscopic level depends on the accurate determination of constitutive parameters of porous structure. Mesoscale simulation can be used for the determination of the above-mentioned constitutive parameters.

- The continuum theory of sintering is applicable for the description of both free and constrained sintering of bilayer systems.
- Difference in chemical composition of adjacent layers has stronger impact on the development of stress and density gradients in comparison with difference in porosity and boundary conditions.

ACKNOWLEDGMENT

The support of Sandia National Laboratory is gratefully acknowledged. This work has been partially supported by the NSF Division of Manufacturing and Industrial Innovation, Grant DMI-9985427 (Program Director Dr. Delcie Durham).

REFERENCES

[1]. V. Tikare, E. Olevsky, and M. Braginsky, Combined macro-meso scale modeling of sintering. Part I: Mesoscale simulation, *this publication*

[2]. E. Olevsky, Theory of sintering : from discrete to continuum. Invited Review, *Mater. Sci. & Eng. R: Reports*

[3]. V.V. Skorohod, Rheological Basis of the Theory of Sintering, Kiev, Naukova Dumka (1972)

[4]. W. Beere, The second stage sintering kinetics of powder compacts, *Acta Metall.*, 23(1), 139-145 (1975)

[5]. R.K. Bordia and G.W. Scherer, Overview No. 70. On constrained sintering II. Comparison of constitutive models, *Acta Metall.*, 36(9), 2399 (1988)

[6]. M.N. Rahaman, R.J. Brook, and L.C. DeJonghe, Effect of shear-stress on sintering, *J. of Amer. Ceram. Soc.*, 69, 53-58 (1986)

[7]. C.H. Hsueh, A.G. Evans, R.M. Cannon, and R.J. Brook, Visco-elastic stresses and sintering damage in heterogeneous powder compacts, *Acta Metall.*, 34, 927 (1986)

[8]. L.C. De Jonghe and M.N. Rahaman, Sintering stress of homogeneous and heterogeneous powder compacts, *Acta Metall.*, 36(1), 223 (1988)

[9]. M.F. Ashby, Background Reading, HIP 6.0, University of Cambridge, Cambridge, U.K. (1990)

[10]. F.B. Swinkels and M.F. Ashby, A second report on sintering diagrams, *Acta Metall.*, 29, 259-281 (1985)

[11]. A.C.F. Cocks, Overview No.117. The structure of constitutive laws for the sintering of fine grained materials, *Acta Metall.*, 42(7), 2191 (1994)

[12]. R.M. McMeeking and L.T. Kuhn, Diffusional creep law for powder compacts, *Acta Mater.*, 40(5), 961 (1992)

[13]. D. Bouvard, and R.M. McMeeking, The deformation of interparticle necks by diffusion controlled creep, *J. Amer. Ceram. Soc.*, 79, 666-672 (1996)

[14]. J. Besson and M. Abouaf, Rheology of porous alumina and simulation of hot isostatic pressing, *J. Amer. Ceram. Soc.*, 75(8), 2165 (1992)

[15]. A.C.F. Cocks and N.D. Aparicio, Diffusional creep and sintering - the application of bounding theorems, *Acta Metall.*, 43(2), 731 (1995)

[16]. H. Riedel, V. Kozak, and J. Svoboda, Densification and creep in the final stage of sintering, *Acta Metall.*, 42(9), 3093 (1994)

[17]. J. Svoboda and H. Riedel, New solutions describing the formation of interparticle necks in solid-state sintering, *Acta Metall.*, 43(1), 1 (1995)
[18]. J. Svoboda, H. Riedel, and R. Gaebel, A model for liquid phase sintering, *Acta Mater.*, 44(8), 3215 (1996)
[19]. C.H. Hsueh, A.G. Evans, R.M. Cannon, and R.J. Brook, Visco-elastic stresses and sintering damage in heterogeneous powder compacts, *Acta Metall.*, 34, 927 (1986)
[20]. K.R. Venkatachari and R. Raj, Shear deformation and densification of powder compacts, *J. of Amer. Ceram. Soc.*, 69(6), 499 (1986)
[21]. M.N. Rahaman, L.C. De Jonghe, G.W. Scherer, and R.J. Brook, Creep and densification during sintering of glass powder compacts, *J. of Amer. Ceram. Soc.*, 70(10), 766 (1987)
[22]. Z.-Z. Du and A.C.F. Cocks, Constitutive models for the sintering of ceramic components - I. Material Models, *Acta Metall.*, 40(8), 1969, (1992)
[23]. Z.-Z. Du and A.C.F. Cocks, Constitutive models for the sintering of ceramic components - II. Sintering of inhomogeneous bodies, *Acta Metall.*, 40(8), 1981, (1992)
[24]. R.M. McMeeking and L.T. Kuhn, Diffusional creep law for powder compacts, *Acta Mater.*, 40(5), 961 (1992)
[25]. A.C.F. Cocks., Inelastic deformation of porous materials, *J. Mech. Phys. Solids*, 37, 693 (1989)
[26]. P. Ponte Castaneda, The effective mechanical properties of nonlinear isotropic composities, *J. Mech. Phys. Solids*, 39, 45 (1991)
[27]. J.M. Duva and P.D. Crow, The densification of powders by power-law creep during hot isostatic pressing, *Acta Metall.*, 40, 1, 31-35 (1992)
[28]. J. Mackenzie and R. Shuttleworth, A phenomenological theory of sintering, *Proc. Phys. Soc.*, 62, 12-B, 833-852 (1949)